HYDROGEN, FUEL CELL & ENERGY STORAGE

Generating electricity using pico hydro-based power plant in Koohrang county, Iran: effect of energy storage type

Mehdi Jahangiri[a,*] | **Ahmad Haghani**[a] | **Heidar Ali Raeisi**[a] | **Ali Mostafaeipour**[b]

[a] Energy and Environment Research Center, Shahrekord Branch, Islamic Azad University, Shahrekord, Iran
[b] Department of Civil and Environmental Engineering, California State University, Fullerton, California, USA
[*] Corresponding author, Email: jahangiri.m@iaushk.ac.ir

Article Information

Article Type
Research Article

Article History
Received: *06 Oct 2023*
Revised: *24 Nov 2023*
Accepted: *16 Dec 2023*
Published Online: *17 Dec 2023*

Keywords
Pico hydro
Reformer
Hydrogen
HOMER

Abstract

Hydropower boasts the capability to consistently generate electricity throughout the year, offering the lowest operating costs and the longest lifespan among renewable energy technologies. Given the aforementioned considerations and the absence of prior investigations into Iran's hydropower potential, this study employs HOMER software to explore the feasibility of supplying electricity to a village comprising 10 households near Koohrang Tunnel in Chaharmahal and Bakhtiari Province, leveraging solar, wind, and hydro turbine renewable energies. Three distinct scenarios, centered around hydro turbine utilization, were examined. These scenarios aimed to provide electricity in off-grid (1st scenario) and grid-connected modes (2nd scenario), as well as to generate electricity and hydrogen in a grid-connected mode (3rd scenario). In the first scenario, the most economically viable design yielded a cost of \$0.187 per kWh of generated electricity, with 99% of the electricity sourced from the hydro turbine and the remaining 1% from a diesel generator. This scenario resulted in a CO_2 emission of 23.2 kg/y. In the second scenario, the most cost-effective option supplied 94% of the electricity from the hydro turbine and the remaining portion from the main grid, at a cost of \$0.033 per kWh. Notably, surplus electricity sold to the main grid facilitated an annual reduction of 1297 kg of CO_2 emissions. The third scenario, which combined the hydro turbine with the main grid, presented the most financially viable option. Here, the costs of per kWh of generated electricity and per kg of produced hydrogen were \$2.012 and \$0.49, respectively.

Cite this article: Jahangiri, M., Haghani, A., Raeisi, H. A., Mostafaeipour, A. (2024). Generating electricity using pico hydro-based power plant in Koohrang county, Iran: effect of energy storage type. DOI: 10.22104/HFE.2024.6680.1287

 Publisher: Iranian Research Organization for Science and Technology (IROST)
DOI: 10.22104/HFE.2024.6680.1287

1 Introduction

Electricity generated from hydroelectric power harnesses the natural flow of rivers through various types of generators. Ideal candidates for hydroelectric power are rivers located in elevated areas [1]. Leveraging the continuous flow of rivers, renewable hydroelectric power stands out for its ability to generate electricity ceaselessly throughout the year, setting it apart from other renewable sources like wind and solar energy [2, 3]. Moreover, it boasts the lowest operating costs and the longest lifespan among renewable energy technologies. Small-scale hydroelectric power plants have minimal environmental impact and do not contribute to pollution unlike coal and oil-based energy resources [4]. To further minimize environmental impact, it's feasible to utilize only a portion of the river's flow.

Hydropower technologies are typically categorized into two main groups: small-scale, which refers to installations generating less than 10 MW, and large-scale, which encompasses those generating more than 10 MW [5]. However, a more detailed classification includes five distinct groups: large-scale (output power exceeding 10 MW), small-scale (output power ranging from 1 to 10 MW), mini (output power between 100 kW and 1 MW), micro (output power between 5 and 100 kW), and pico (output power less than 5 kW) [1].

Hydroelectric power stands as the largest and singularly established renewable energy source employed commercially worldwide for power generation. Its potential utilization spans approximately 150 countries, with feasibility present in over 100 nations [2]. Notably, the utilization of hydroelectric power predates and surpasses that of other renewable energy sources in terms of both scale and longevity. Currently, hydroelectric power contributes around 17% of global production capacity and accounted for approximately 20% of energy production in the mid-twentieth century [6]. Consequently, its operational history and productivity outweigh those of alternative renewable energy sources [7].

In 2013, approximately 16% of the world's total energy consumption was met by 100 GW of hydroelectric power [8]. Noticeably, the developed countries heavily rely on hydroelectric power for electricity generation, with examples such as 10% of electricity in the United States and over 99% in Norway sourced from this renewable energy [9]. Furthermore, the developing nations, particularly those situated along the equatorial belt, also leverage hydroelectricity to meet their energy demands. For instance, in 2004, Malaysia derived about 11% of its electricity from hydroelectric sources [10]. While large-scale hydroelectric systems dominate the landscape, smaller-scale hydropower technologies are better suited for supplying energy to remote regions [1]. Indeed, the viability of hydroelectric power in remote villages hinges on the accessibility of resources. While it has the potential to offer some of the lowest energy costs, its feasibility is contingent upon the availability of suitable resources [11].

In 2008, Nfah et al. conducted a simulation using HOMER software to address the electricity needs of remote villages in Cameroon, aiming to provide 110 kWh/day [12]. In the most economically favorable scenario, the energy cost amounted to \$0.296 per kWh. This scenario entailed a system comprising a 14 kW water turbine, a 15 kW gas generator, and a 36 kWh battery. The researchers concluded that for discharge rates exceeding 200 L/s in southern Cameroon, a hybrid hydro turbine system, and for solar radiation surpassing 5.55 kWh/m^2/day in northern Cameroon, a photovoltaic hybrid system would represent the most cost-effective options.

In 2009, Boustani conducted an assessment of the potential for a small hydroelectric power plant in the Sisakht region of Yasuj [13]. The power plant under investigation was constructed on the Polkolo River. This power plant, which consists of 9 interconnected power plants, has a total head of 1100 m, a flow rate of 2.5 m^3/s, and an annual energy production of 105.5 million kWh. In 2009, Nfah and Ngundam utilized simulated hydro turbine/solar cell/biogas generator systems employing HOMER software [14]. Their objective was to provide 73 kWh of electricity daily to remote villages in Cameroon. Their findings indicated that the hydro turbine/battery/biogas generator configuration, requiring a minimum water discharge of 92 L/s in southern Cameroon, was more cost-effective than a solar cell/battery/biogas generator setup necessitating a minimum radiation of 5.55 kWh/m^2/day in northern Cameroon. Additionally, they emphasized that investing in biogas systems alongside other renewable energies could play a pivotal role in the poverty reduction programs of Cameroon's National Energy Agency.

In 2014, Sen and Bhattacharyya utilized the HOMER software to determine the most effective combination of renewable energy sources for generating electricity in a remote Indian village lacking access to the national grid [15]. Their analysis incorporated renewable resources such as solar, wind, hydropower, and biomass, comparing the outcomes with the cost of grid electricity. The optimal configuration identified comprised 14% solar cells, 76% hydropower, and 10% biomass generators, fulfilling the village's annual requirement of 246, 382 kWh. The total net presents cost amounted to \$673, 147, with an energy cost of \$0.42/kWh.

In 2015, Teixeira [16] investigated the viability of implementing a hydro-solar hybrid system connected to the national grid at a water supply dam in southern Brazil, employing the HOMER software. The findings revealed that 227 kW of electricity was supplied by hydro turbines, while an additional 60 kW was provided by solar cells, indicating a less economical outcome. The initial cost was \$1715.83/kWh, with an associated energy cost of \$0.059/kWh. Comparatively, the price of electricity from the national grid stood at \$0.16/kWh.

In 2017, Ajao et al. [17] probed a small-scale hydroelectric power plant located in Bakolori, Nigeria, with the aim of evaluating the feasibility of upgrading its electromechanical equipment. Their study concluded that outfitting the power plant with new production equipment could bolster its production capacity by 3.2 MW.

Given that electricity generation often falls short of demand, the utilization of small hydroelectric power stations emerges as a potential solution to address this disparity. In 2017, Hammid et al. [18] delved into the application of artificial neural networks to forecast the performance of a standalone hydro turbine facility associated with the Diyala Dam. Leveraging 3570 sets of experimental data, they trained the neural network model. Ultimately, they achieved a correlation exceeding 0.96 between predicted and actual variables, underscoring the high precision and accuracy of the network.

Based on the mentioned contents and the studies done by others, the discussion of various energy storage types has not been addressed in none of them and mostly focused on rural and remote areas. Taking into account the substantial energy demand in Iran and after reviewing available literature, it's noteworthy that there has been a lack of research on the utilization of small hydropower plants within the country. Thus, the current study aims to fill this gap by applying HOMER software to simulate a hybrid Pico hydro turbine/solar cell/diesel generator system in the Koohrang area of Chaharmahal and Bakhtiari Province. Alongside economic assessments and cost estimations, the study also evaluates the environmental impact by assessing the pollutants emitted through the use of the diesel generator.

2 Pico hydropower plant and its benefits

A Pico hydroelectric power plant typically generates electrical power up to 5 kW using natural water flow. These systems are capable of meeting the electricity demands of a limited number of homes or small commercial and industrial communities. Due to their reliance on natural water flow and absence of fuel-related costs, Pico hydroelectric power plants are considered an economical energy source, making them viable for deployment worldwide, particularly in developing nations. Pico hydroelectric systems complement photovoltaic solar systems, as water flow and hydroelectric power are often at their peak during winter months, coinciding with lower solar energy availability.

According to statistics from the Iran Renewable Energy and Energy Efficiency Organization (SATBA) [19, 20], as of September 2021, small hydropower accounted for 11.58% of the total renewable electricity generation in Iran, amounting to 904.07 MW. Notably, the majority of small hydropower plants in the country operate on a mini- and micro-scale, with no existing plants operating on a pico-scale.

3 Hydrogen energy and its storage

Hydrogen stands out as one of the most promising alternatives for energy, although it doesn't exist freely in nature. Similar to electricity, hydrogen is not considered a primary energy source; rather, it's regarded as a secondary form of energy derived from natural and biological resources. Forecasts suggest that hydrogen will assume a significant role in future energy scenarios across various sectors [21]. Despite its complexity when integrated with other energy sources, research underscores hydrogen as an exceptional energy carrier with extensive benefits, poised to substitute fossil fuels in the near future. Anticipations suggest that hydrogen will emerge prominently after 2030 [22, 23].

When comparing energy storage capabilities, hydrogen storage surpasses lithium-ion batteries, storing more energy for the same amount produced. Moreover, the relatively low cost of materials required for compressed hydrogen storage, contrasted with the higher cost associated with storing electric charge in batteries, positions hydrogen storage as a superior alternative to battery storage [24].

The promising prospects of "hydrogen energy" have garnered considerable interest in Iran, a nation endowed with abundant and diverse energy sources [25]. However, despite extensive research conducted across various regions of Iran exploring the potential for hydrogen production from various sources [26–32], only a few applied projects have been realized. Among these projects, the most noteworthy is the Taleghan Solar Hydrogen Pilot Power Plant developed by SATBA.

The share of renewables in the total energy demand is projected to rise to 36% by 2025 and further to 69% by 2050, with hydrogen accounting for 11% by 2025

and 34% by 2050. With adequate support for hydrogen production technology, the utilization of crude oil and charcoal is expected to decrease to 40.5% and 36.7% by 2030, respectively [33].

In the current study, hydrogen production is conducted via water electrolysis, as illustrated in Figure 1. The energy required for electrolysis is sourced from wind, solar, and hydro power. The materials, method, and energy sources utilized in this study for hydrogen production are highlighted in yellow in Figure 1.

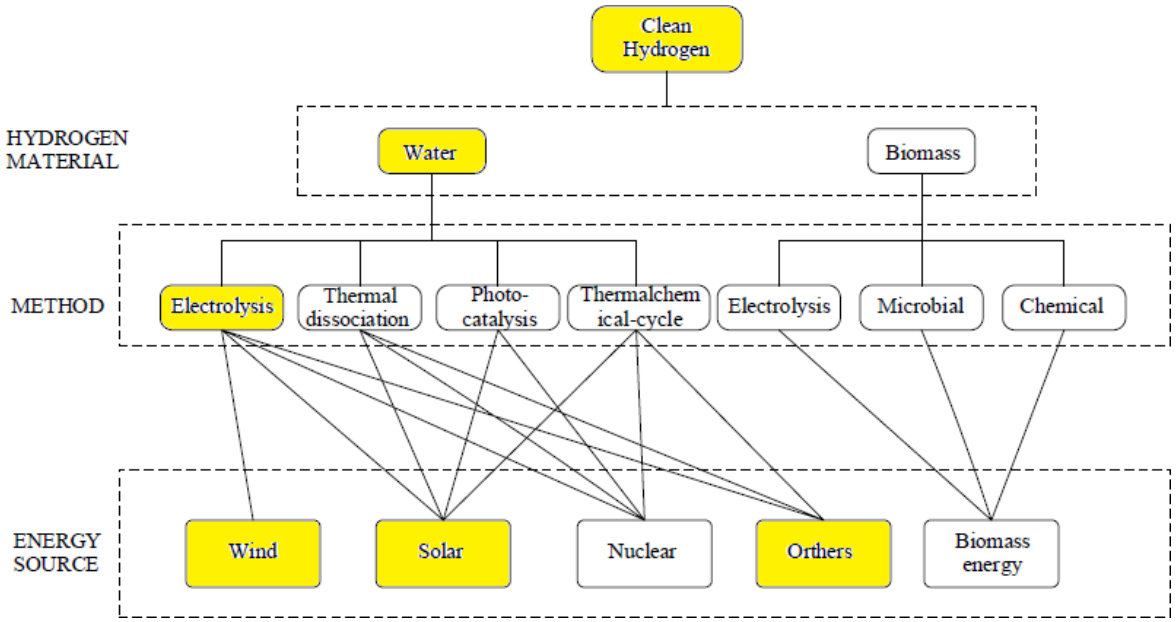

Fig. 1. Different hydrogen production technologies [34].

4 Benefits of grid-connected systems

From a broad perspective, one of the advantages of grid-connected systems lies in the seamless transmission of power to the power grid and utility. In these systems, when the solar array produces surplus electricity beyond the household or business's consumption, the excess electricity is provided to the grid for free. Conversely, if consumption exceeds production, consumers are only charged for the excess electricity they consume. Generally, grid-connected renewable energy systems are characterized by trade, sale, and revenue generation. In this setup, the power utility facilitates both power production and consumption, ensuring that consumers have access to electricity even during times when renewable energy sources cannot fully meet demand. During such periods, the power grid supplies the required load as needed [35].

5 Study area

The Koohrang Tunnel, situated at coordinates 32°08′53.96″N 50°26′07.57″E in Chaharmahal and Bakhtiari province, serves as a conduit designed to convey water from the Marbor River (Koohrang Water) to Zayanderud near Chelgerd or Koohrang city in Iran's Chaharmahal and Bakhtiari province. Regarded as one of the most picturesque natural attractions in the Koohrang region, the Koohrang Tunnel offers captivating views throughout the seasons, as depicted in Figures 2 and 3. These images serve to illustrate the proposed location for installing the hydro turbine, showcasing the flow rate during both summer and winter seasons, as well as highlighting the water head and the potential for power generation.

Fig. 2. Koohrang Tunnel in the Winter.

Fig. 3. Koohrang Tunnel in the Summer.

Given the considerable height and slope of the tunnel, along with the optimal width and water flow conditions, the Gorlov Helical hydro turbine has been selected for use in this project. Positioned in the path of water flow, this turbine rotates and generates electricity as water passes through it. Importantly, the continuous flow of water ensures that it remains dynamic and does not stagnate, mitigating any potential environmental concerns associated with stagnant water.

6 Materials and methods

HOMER software, acronym for "Hybrid Optimization Model for Electric Renewables", is a robust tool developed by the US National Renewable Energy Laboratory. It serves to assess the feasibility of implementing renewable energy-based systems by identifying the most cost-effective solutions and lowest net present cost over the course of 8760 hours per year. The software is chosen for this study due to its accessibility (it is freely available) and its ability to streamline the design process of renewable energy-based systems, whether for off-grid or grid-connected applications. HOMER is renowned for its capability to conduct comprehensive techno-economic and environmental analyses concurrently, on an hourly basis, throughout a one-year period [36]. The flowchart depicted in Figure 4 illustrates the process of implementing analyses within the software. As shown, HOMER takes various data inputs such as technical specifications, climate data, load requirements, economic parameters, search space constraints, and equipment specifications. Subsequently, through simulation and optimization of feasible scenarios, the software organizes the results in ascending order based on net present cost.

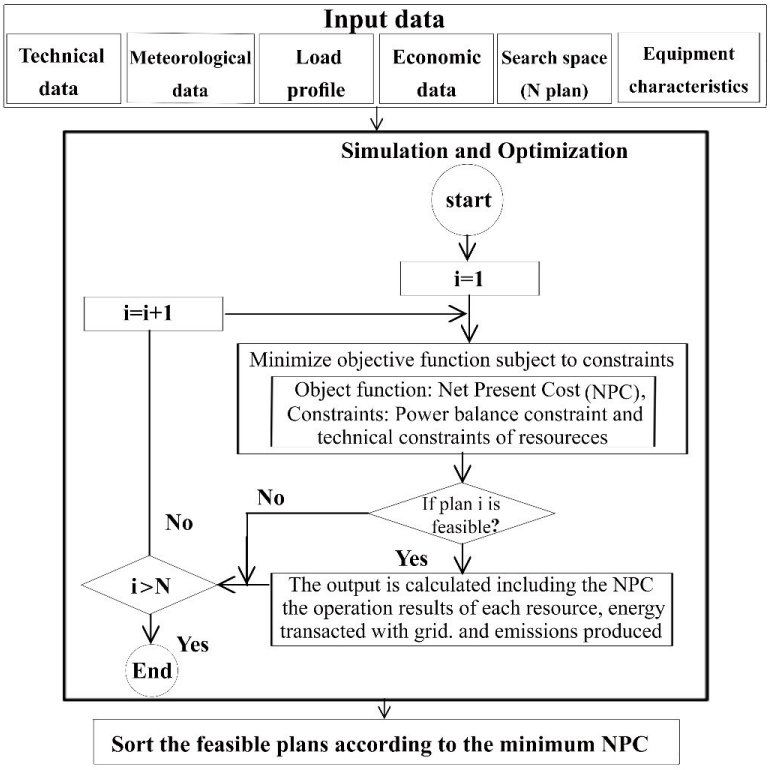

Fig. 4. Comprehensive flowchart of analyses implemented in HOMER

HOMER models solar cells independently of their temperature and the voltage they are exposed to. The software calculates the power production of solar cells using equation (1) [37]

$$P_{\mathrm{PV}} = f_{\mathrm{PV}}\, Y_{\mathrm{PV}}\, \frac{I_T}{I_s}\,, \tag{1}$$

where f_{PV}, Y_{PV}, I_T, and I_s are the PV derating factor, installed capacity of the solar cells, global solar radiation incident of the surface of the PV array, and the amount of radiation used to rate the capacity of the PV array, respectively.

HOMER computes the average power output of the wind turbine using equation (2) [38]:

$$P_{\mathrm{wind}} = \frac{1}{2}\,\tau\rho\, C_p\, A \sum_{x=1}^{j} f_{(v)} v_x^3\,, \tag{2}$$

where τ, ρ, C_p, A, $f_{(v)}$, j and v are the analysis time (one year), air density, the wind generator capacity factor, area swept by the blades, Weibull distribution, data class numbers, and wind speed, respectively.

In renewable energy systems, batteries are employed when energy sources are unavailable or insufficient. HOMER determines the required number of batteries for each scenario using equation (3) [39]:

$$N_{\mathrm{batteries}} = \frac{E_d\, n_d}{V_{\mathrm{battery}} \times \mathrm{AH} \times \mathrm{DOD}}\,, \tag{3}$$

where E_d, n_d, V_{battery}, AH, and DOD are the daily energy required, number of days when backup power is required, battery voltage, battery's amp-hour rating, and battery's depth of discharge, respectively.

The size of the power converter is established relative to the size of renewable equipment generating DC power to optimize the energy extracted by the converter. The constant R is commonly employed to denote the ratio of the size of renewable equipment producing DC power to the size of the power converter, and it is defined as equation (4) [40]:

$$R = \frac{\text{The size of the DC electricity producer's renewable equipment}}{\text{The inverter size}}\,. \tag{4}$$

The size of the power converter is always smaller than or equal to the size of renewable equipment producing DC power ($R \geq 1$) because DC power equipment typically operates below its rated power output for extended periods. Consequently, opting for oversized power converters is often economically unjustifiable [41]. The performance of a diesel generator is delineated by its fuel consumption at each time interval, as quantified by equation (5) [42]:

$$F_D = aT_G + bP_G\,, \tag{5}$$

where a, T_G, b, and P_G are fuel curve intercept coefficient, diesel generator rated capacity, fuel curve slope, and power generated by the diesel generator at each time step, respectively. The equation provided is utilized to determine the efficiency of the diesel generator, as expressed by equation (6) [43]:

$$\eta_G = \frac{3600 P_G}{\rho_D\, F_D\, \mathrm{LHV}_D}\,, \tag{6}$$

where ρ_D, F_D, and LHV_D parameters are diesel density, hourly fuel consumption, and lower heating value of diesel, respectively. HOMER computes the electrical generation of the hydro turbine using equation (7) [44]:

$$P_{\mathrm{hyd}} = \frac{\eta_{\mathrm{hyd}}\, \rho_{\mathrm{water}}\, Q_{\mathrm{turbine}}\, g\, h\, (1 - f_h)}{10^3\ \mathrm{w/kW}}\,, \tag{7}$$

where η_{hyd}, ρ_{water}, Q_{turbine}, g, h, and f_h parameters are hydro turbine efficiency, water density, turbine's volumetric flow rate, gravitational acceleration of earth, the available head, and head losses in the pipe, respectively.

If the net monthly electricity generation is known, HOMER can determine the total annual cost of energy using equation (8) where $E_{\text{net grid purchases},i,j}$, $c_{\mathrm{power},i}$, $c_{\mathrm{sellback},i}$ parameters are net grid power purchases in month j during which rate i is applied, grid power price for rate i, and grid sellback price for rate i, respectively [45].

Electrolyzer efficiency is the efficiency with which the electrolyzer converts electricity into hydrogen and HOMER calculates it by the equation (9) [46]. The reformer efficiency denotes the proportion of fuel converted into hydrogen and is computed in HOMER using equation (10) [46].

$$C_{\text{grid energy}} = \sum_{i}^{\text{rates}} \sum_{j}^{12} \begin{cases} E_{\text{net grid purchases},i,j} \times c_{\mathrm{power},i} & E_{\text{net grid purchases},i,j} \geq 0 \\ E_{\text{net grid purchases},i,j} \times c_{\mathrm{sellback},i} & E_{\text{net grid purchases},i,j} < 0 \end{cases}\,, \tag{8}$$

$$\eta_{\mathrm{electrol}} = \frac{\text{The energy content (based on HHV) of the hydrogen produced}}{\text{The amount of electricity consumed}}\,, \tag{9}$$

$$\eta_{\mathrm{ref}} = \frac{\text{The energy content (based on LHV) of the hydrogen}}{\text{The energy content (based on LHV) of the fuel}}\,. \tag{10}$$

To model a system that produces its required hydrogen through the electrolysis of excess electrical production, a hydrogen tank is necessary to store the hydrogen for various applications. The hydrogen tank autonomy, quantifying the ratio of the energy capacity of the hydrogen tank to the electrical load, is calculated using equation (11) [47]:

$$A_{\text{htank}} = \frac{Y_{\text{htank}}\,\text{LHV}_{\text{H}_2}(24\,\text{h/d})}{L_{\text{prim.ave}}\,(3.6\,\text{Mj/kWh})}\,, \tag{11}$$

where Y_{htank}, LHV_{H_2}, and $L_{\text{prim.ave}}$ are hydrogen tank rated capacity, the lower heating value of hydrogen fuel, and average primary load, respectively.

HOMER obtains optimal solutions based on the least cost of energy and net present cost, both of which are derived by the equations (12) and (13) [48]:

$$\text{COE} = \frac{C_{\text{A.cap}} + C_{\text{A.rep}} + C_{\text{A.O\&M}}}{E_s}\,, \tag{12}$$

$$\text{NPC} = \frac{C_{\text{A.cap}} + C_{\text{A.rep}} + C_{\text{A.O\&M}}}{\frac{\left(\frac{i-f}{1+f}\right)\left(1+\frac{i-f}{1+f}\right)^n}{\left(1+\frac{i-f}{1+f}\right)^n - 1}}\,, \tag{13}$$

where $C_{\text{A.cap}}$, $C_{\text{A.rep}}$, $C_{\text{A.O\&M}}$, E_s, i, f, and n are annual capital cost, annual replacement cost, the annual cost of components' operating and maintenance, energy supplied during a year, real interest rate, annual inflation rate, and the number of years, respectively.

7 Required data and studied systems

Given that the focus of the present study was on various energy storage types, grid electricity, battery and hydrogen were used for this purpose. Table 1 presents the prices, sizes, lifetimes, and other pertinent information regarding the components utilized in the simulation. It's worth noting that the fuel price was \$0.09 [49], with an 18% annual interest rate [50], for a project lifetime of 25 years. Figures 13 to 15 depict monthly data for solar radiation, river flow rate, and wind speed, respectively. As evident from the Figures, the maximum values for solar radiation, wind speed, and discharge flow rate occur in June, July, and June, respectively, with values of 7.71 kWh/m^2/day, 5 m/s, and 13080 L/s. Additionally, the average annual values for solar radiation, wind speed, discharge flow rate, and clearness index are 5.061 kWh/m^2/day, 4.252 m/s, 3917.1 L/s, and 0.592, respectively.

The climatic data used were obtained from the Meteorological Organization of Chaharmahal and Bakhtiari Province (Figures 13 and 15) and the Regional Water Company of Chaharmahal and Bakhtiari Province (Figure 14), and their accuracy has been fully confirmed. If similar data are available for any other point or climate in the country, the scenarios of present research can be implemented for that location.

Table 1. Simulated hybrid power plant information.

Component	Purchase ($)	Replacement ($)	Operating & Maintenance ($)	Lifetime	Size of equipment
Wind Turbine BWC XL.1 (1 kW) [51]	3900	3900	100	25 year	see Figure 5
PV (1 kW) [52]	6900	6900	0	25 year	see Figure 6
Battery Surrette 6CS25P [53]	1200	1170	10	9645 Wh	see Figure 7
Hydro turbine [54]	1700	500	51	30 year	1 kW
Converter (1 kW) [55]	800	700	100	15 year	see Figure 8
Generator (1 kW) [56]	200	200	0.5	15000 hour	see Figure 9
Electrolyzer (8 kW) [52]	2700	2700	3	15 year	see Figure 10
Reformer (8 kg/hr) [52]	3200	3200	4	25 year	see Figure 11
Hydrogen Tank (8 kg) [52]	3100	3100	4	25 year	see Figure 12

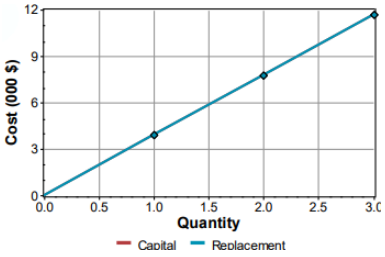

Fig. 5.

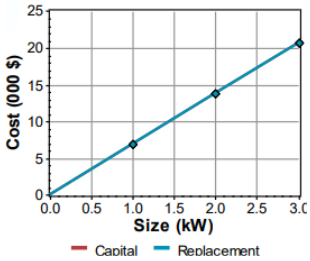

Fig. 6.

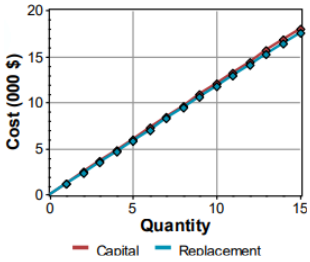

Fig. 7.

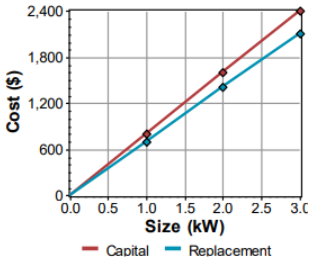

Fig. 8.

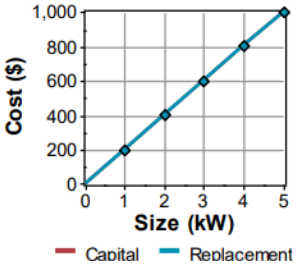

Fig. 9.

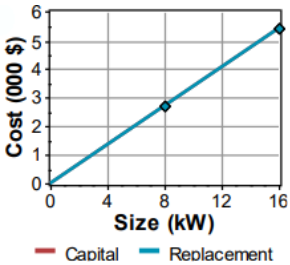

Fig. 10.

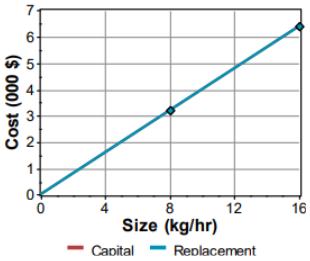

Fig. 11.

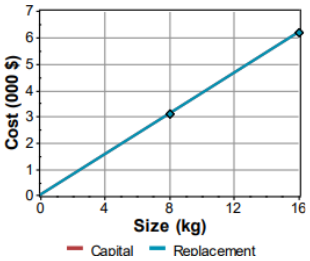

Fig. 12.

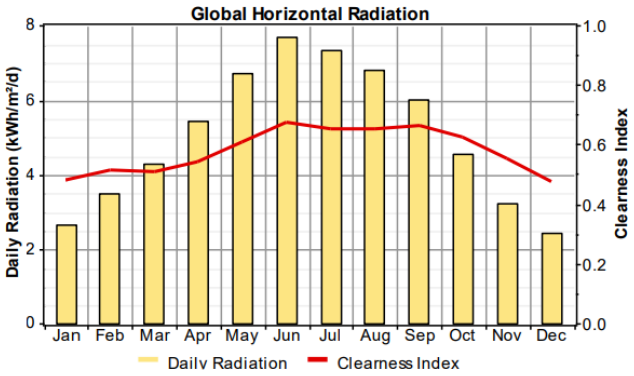

Fig. 13. Solar radiation in the studied area.

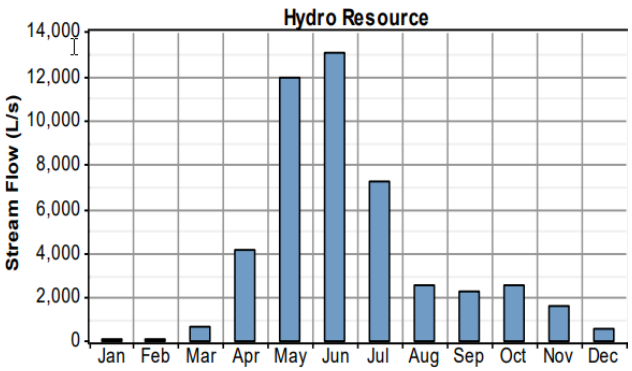

Fig. 14. Flow rate of Koohrang tunnel.

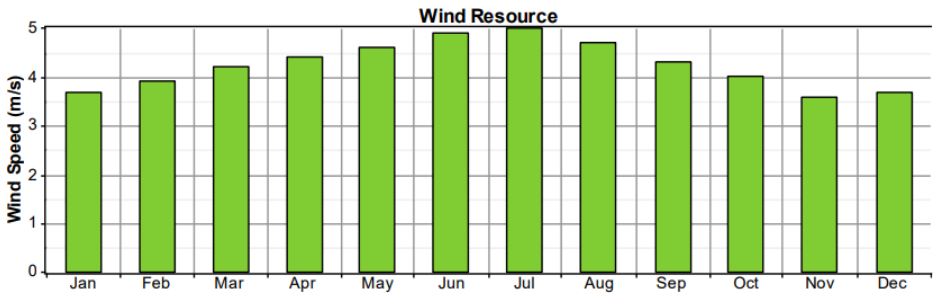

Fig. 15. Wind speed in the studied area.

The real electric consumption data pertains to a village comprising 10 households located near the river, as illustrated in Figure 16. Leveraging the weather conditions and geographic location of the site, the software can extrapolate electricity consumption for other months, assuming 24-hour electricity consumption per day.

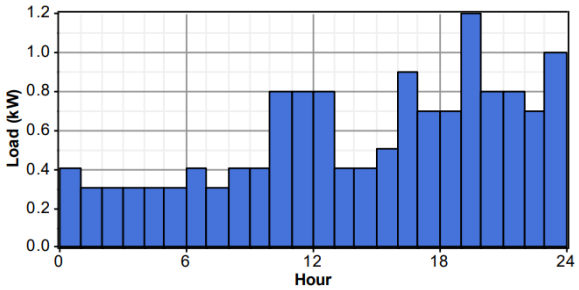

Fig. 16. Daily power consumption profile.

As evident from the 24-hour electricity consumption profile, peak hours occur between 10-13 and 16-24, with the highest load reaching 1.2 kW at 19-20. It's worth noting that electricity usage is predominantly for lighting purposes from midnight to 08:00.

The hydrogen requirements for 24 hours over the course of 12 months are depicted in Figure 17 [52]. On average, the daily and hourly quantities of hydrogen required over a year are 85 kg and 3.54 kg, respectively, with a maximum hourly demand of 11.5 kg. This Figure illustrate that hydrogen is primarily needed during peak hours from 16:00 to 19:00, while the demand is lowest during the period from 23:00 to 6:00.

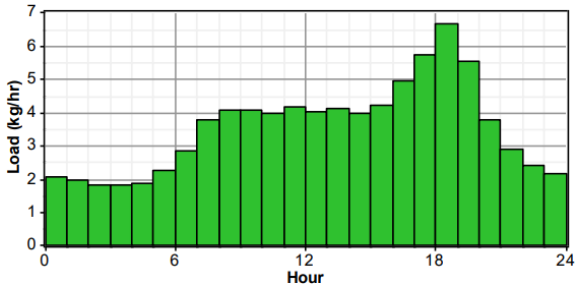

Fig. 17. Daily profile of required hydrogen

The hybrid system under study is interconnected with the main grid, enabling it to procure electricity from and sell its surplus electricity to the grid. Since electricity is priced differently during periods of low-load (23:00-08:00), high-load (16:00-23:00), and mid-load (08:00-16:00), three distinct schemes are adopted for selling and purchasing electricity to and from the grid. Uniform prices are assumed for both selling and buying electricity, with rates set at \$0.12, \$0.07, and \$0.05 per kWh during high-load, mid-load, and low-load periods, respectively. Moreover, considering CO_2 as the primary pollutant, an emission factor of 632 g of CO_2 per kWh of main grid electricity has been accounted for. Additionally, a capacity of 1000 kW has been designated for buying and selling to and from the main grid [57].

Taking into account the inclusion of a diesel generator in the studied hybrid systems, the emissions quantity per liter of diesel is provided in Table 2 [58]. In this study, the intercept coefficient and slope coefficient of 0.08 have been adopted for the diesel generator, based on which the power output diagram ($\eta_{\text{gen}} \approx 65\%@100\%$ of output) as a function of efficiency has been derived. The dispatch strategy for the diesel generator in this study follows a cycle charging approach, wherein the generator operates at full output power, and any surplus electricity generated is utilized to either charge the battery or support the electrolyzer.

Table 2. Pollutants emitted due to diesel consumption [58].

Pollutant type	Amount
Carbon monoxide	6.5 g/L
Unburned hydrocarbons	0.72 g/L
Particulate matter	0.49 g/L
Proportion of fuel sulfur converted to PM	2.2%
Nitrogen oxides	58 g/L

A schematic depiction of the hybrid systems utilized is illustrated in Figure 18. As observed, three primary scenarios were assessed, encompassing off-grid electricity generation, grid-connected electricity generation, and grid-connected simultaneous electricity and hydrogen generation. In the off-grid mode, batteries serve as a backup to store excess electrical production during periods of low-load and utilize it during high-loads. Additionally, given that renewable energy sources such as wind, solar, and hydropower may not consistently meet the energy demands of the village, a diesel generator has been incorporated to address emergency conditions.

8 Results and discussion

Validation of the present study was conducted using wind speed data from the Lutek station. Figure 19 depicts a comparison between the Weibull function derived in this research and that drawn by Teimourian et al. [59]. The data utilized in Teimourian et al. were obtained through curve-fitting on wind energy data, resulting in parameters of $c = 7.22$ and $k = 1.6$, using an analytical method. In the present research conducted using HOMER software, the parameters derived from

curve-fitting are $c = 7.36$ and $k = 1.97$. The choice of the Weibull function for validation is due to its potential to measure and fit real wind probabilities. The comparison depicted in Figure 19 demonstrates good agreement between the results of the Weibull function from the present study and those of Teimourian et al.

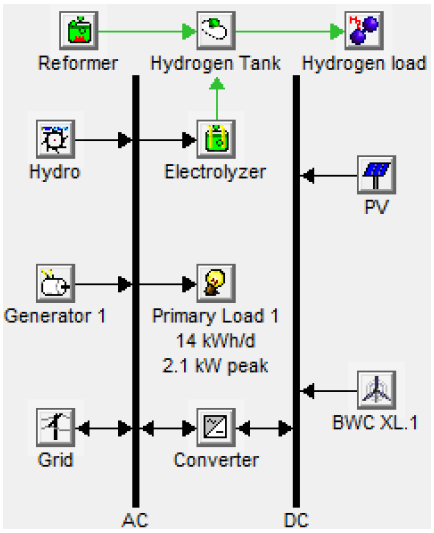

(a)

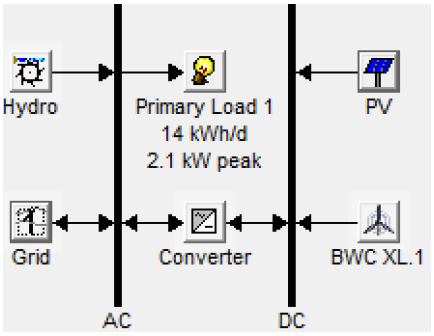

(b)

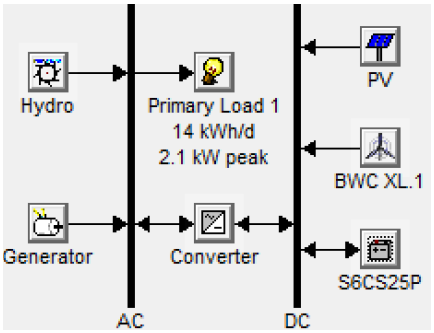

(c)

Fig. 18. Schematic representation of the studied hybrid system: (a) grid-connected simultaneous production of electricity and hydrogen, (b) grid-connected electricity generation, (c) off-grid electricity generation.

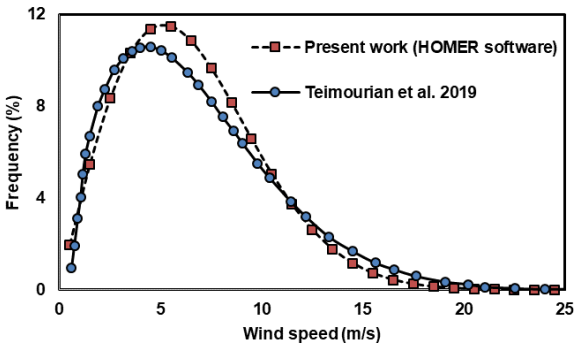

Fig. 19. Validation of HOMER software results compared to previous work using the Weibull function.

8.1 Scenario no. 1: Off-grid power generation

In this scenario, which utilizes batteries for energy storage, a diesel generator, water turbine, PV, and wind turbine have been used for electricity generation. From the results obtained for the first scenario detailed in Table 3, the most economically optimal condition is achieved with the hydro turbine-diesel generator setup, where the price per kWh of generated electricity and net present cost amount to \$0.187 and \$5184, respectively. Additionally, annual CO_2 emissions attributable to the use of the diesel generator is 23.2 kg in total, resulting from the consumption of 9 L of diesel per year during 67 hours of diesel generator operation. As illustrated in Figure 20, in this scenario, 99% of the electricity (7176 kWh/y) is generated by the hydro turbine, with the diesel generator predominantly required during June and September. Consequently, there is an excess electricity production of 1838 kWh/y, as depicted in Figure 21 on a monthly basis. From this Figure, it's evident that a surplus of at least 0.35 kW of electricity is generated daily, with May registering the highest quantity of excess electricity production (0.78 kW).

In this scenario, if the generator is omitted and the entire electricity is to be produced solely by the hydro turbine, the addition of a battery is required. This adjustment increases the cost per kWh of electricity generated by 20% compared to the optimal state. Additionally, as summarized in Table 3, the combined utilization of both hydro and wind turbines in the studied hybrid system leads to a cost per kWh of generated electricity that rises by 83.4% compared to the optimal state. Furthermore, this cost escalation increases to 131% for the combined application of a solar array and hydro turbine.

The results obtained for this scenario highlight the superiority of the system based on a wind turbine over the one based on a solar array. Furthermore, if no hy-

dro turbine is utilized in this scenario, the optimal configuration involves employing a wind turbine, a diesel generator, three batteries, and an electric converter, resulting in a cost of \$0.894 per kWh of electricity generated. However, only 16% of the consumed power is produced by the wind turbine in this configuration. Additionally, this particular setup generates 2112 kg of CO_2 annually.

Table 3. Simulation results for the first scenario.

Components	Total NPC (\$)	COE (\$/kWh)	Ren. Frac. (%)	Excess electricity (kWh/yr)	CO_2 emission (kg/yr)
Battery, Converter, Diesel generator, Hydro turbine	5184	0.187	99	1838	23.2
Battery, Converter, Hydro turbine	6219	0.224	100	1781	0
Battery, Converter, Diesel generator, Hydro turbine, Wind turbine	9521	0.343	≈ 100	2869	10.8
Battery, Converter, Diesel generator, Hydro turbine, PV cell	11969	0.432	≈ 100	3700	10.4
Battery, Converter, Diesel generator, Wind turbine	24808	0.894	20	≈ 0	2112

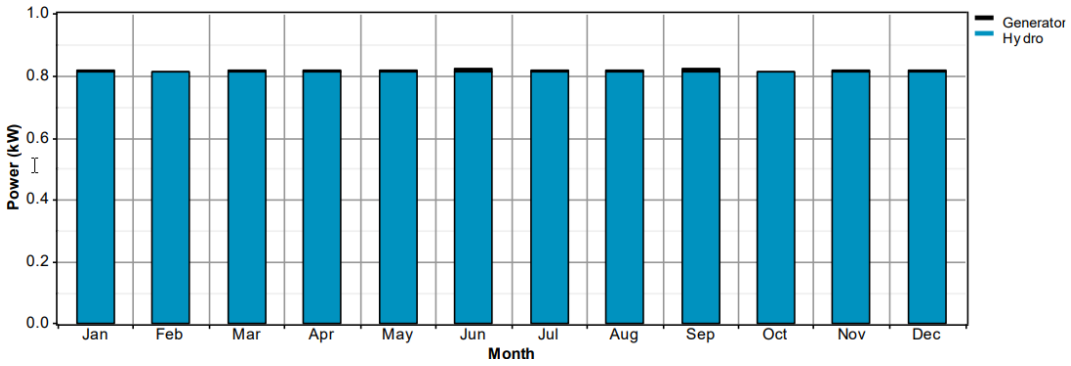

Fig. 20. Monthly average electric production for the optimal state in the scenario 1.

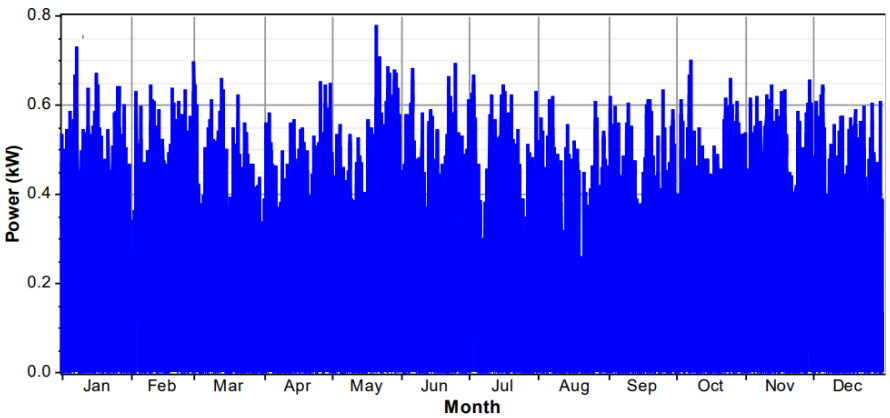

Fig. 21. Excess electricity.

8.2 Scenario no. 2: Grid-connected power generation

In this scenario, which uses grid electricity as an energy storage, the national grid has been used alongside a hydro turbine, PV, and wind turbine for electricity generation.

The results for the second scenario are detailed in Table 4. In this scenario, considering that excess electrical production is sold to the grid during low-loads and power is purchased from the main grid during high-loads, battery storage has not been utilized. Furthermore, since the system is connected to the main grid, no surplus electricity remains.

The optimal configuration for this scenario involves the use of a hydro turbine in conjunction with the main grid, resulting in a price per kWh of electricity and a total net present cost of $0.033 and $1351, respectively. In this most optimal configuration, as depicted in Figure 22, 94% of the electricity production (7126 kWh/y) is generated by the hydro turbine, while the remaining portion is supplied by the main grid.

Table 4. Simulation results for the second scenario.

Components	Total NPC ($)	COE ($/kWh)	Ren. Frac. (%)	CO_2 emission (kg/yr)
Hydro turbine, Grid	1351	0.033	94	−1297
Grid	2376	0.086	0	3206
Hydro turbine, Grid, Wind turbine, Converter	6816	0.150	96	−1844
Grid, Wind turbine, Converter	7841	0.280	18	2659
Hydro turbine, Grid, PV cell, Converter	9009	0.182	96	2325
Grid, PV cell, Converter	10034	0.346	31	2178

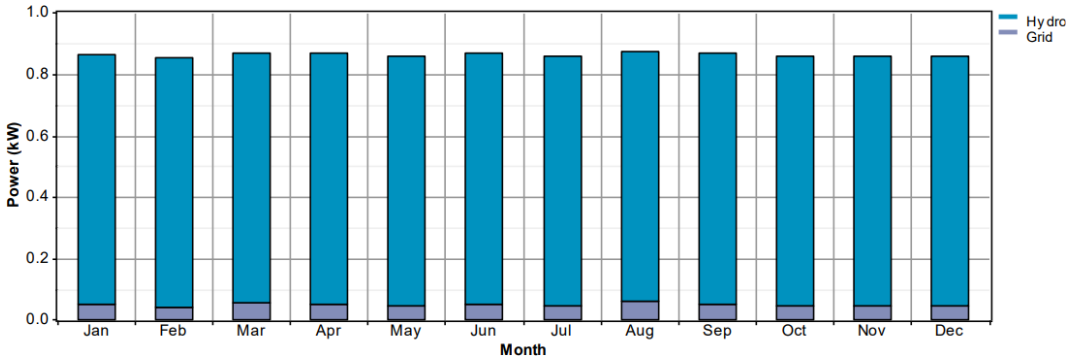

Fig. 22. Monthly average electric production for the optimal state in the scenario 2.

The amounts of electricity sold/bought to/from the main grid over the course of a year are summarized in Table 5. Notably, the highest and lowest amounts of electricity bought from the grid are 46 kWh in August and 28 kWh in February, respectively. Similarly, the highest and lowest amounts of electricity sold to the main grid are 221 kWh in May and 198 kWh in August, respectively. From the results presented in Table 5, it is evident that the amount of electricity sold to the main grid surpasses that bought for all 12 months of the year. In total, the annual amounts of electricity bought and sold to the main grid are 437 kWh and 2490 kWh, respectively. It's worth noting that, since 632 g of CO_2 is produced per kWh of electricity generated by the main grid, selling the renewable electricity produced by hydropower to the main grid results in a saving of 1297 kg of CO_2 annually. Additionally, it is observed that during peak load periods, the electricity sold to the main grid exceeds that bought only in February and October. At peak demand, there is an annual net requirement of 39 kW to be bought from the main grid. Conversely, during mid- and low-load periods, the amount of electricity sold to the main grid exceeds that bought from it for all months. For these periods, the annual net amounts of electricity sold to the main grid are 736 kWh and 1356 kWh, respectively.

Table 5. Electricity exchange with national electricity grid for the optimal state in scenario 2.

Month	Energy purchased (kWh)			Energy sold (kWh)			Net purchases (kWh)		
	Peak	Normal	Off-Peak	Peak	Normal	Off-Peak	Peak	Normal	Off-Peak
Jan	24	7	6	21	74	122	3	−67	−116
Feb	18	5	5	20	68	114	−2	−63	−109
Mar	25	9	8	18	64	120	7	−55	−112
Apr	24	7	7	19	67	117	5	−60	−110
May	23	5	7	22	73	126	2	−68	−119
Jun	24	8	6	19	65	117	5	−57	−110
Jul	24	5	6	22	70	122	2	−65	−116
Aug	28	9	8	17	64	117	11	−54	−109
Sep	23	7	8	18	65	117	5	−58	−110
Oct	21	6	6	23	68	120	−2	−62	−114
Nov	22	5	5	20	69	121	2	−64	−116
Dec	23	6	7	23	69	121	0	−63	−114
Annual	280	79	78	242	814	1434	39	−736	−1356

Figure 23 provides a summary of the annual costs for the best option in the second scenario. It illustrates that \$362 is spent annually on the purchase and operation of the hydro turbine, while the annual revenue generated by selling electricity to the grid amounts to \$115. Consequently, the annual net cost totals \$247. Notably, since the useful lifetime of the hydro turbine exceeds that of the project, and no diesel is consumed, the replacement and fuel costs are depicted as zero in Figure 23.

The second-best option in the second scenario, as indicated by the results in Table 4, involves utilizing the main grid, incurring a cost of \$0.086 per kWh of electricity generation. This cost is approximately 1.26 times higher than that of the optimal configuration for this scenario. In this setup, the entire 5073 kWh of required electricity annually is supplied by the main grid, resulting in the production of 3206 kg of CO_2 pollutants annually. Similar to the first scenario, the results presented in Table 4 for the second scenario highlight the superiority of wind potential over solar potential in the studied area. Specifically, the prices per kWh of electricity produced by wind turbine-hydro turbine-main grid and solar array-hydro turbine-main grid hybrid systems are \$0.15 and \$0.182, respectively.

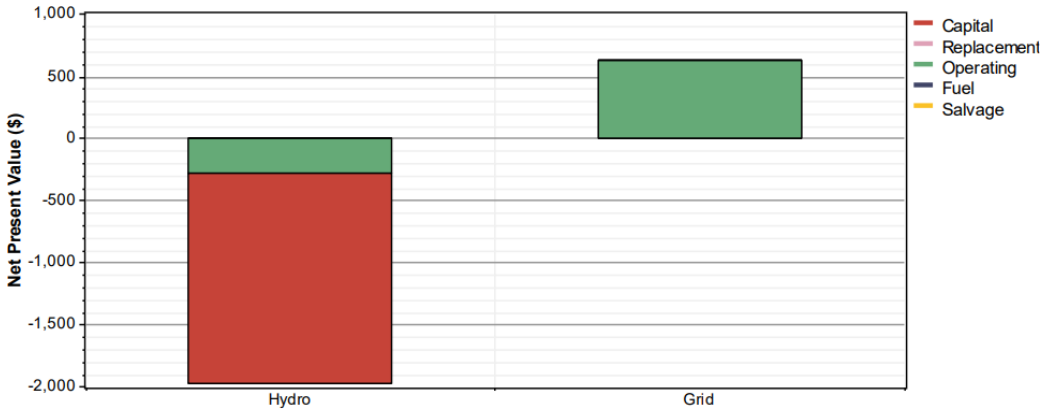

Fig. 23. Annualized cash flow summary for the optimal state in scenario 2.

As depicted in Figure 24, in the wind turbine-hydro turbine-main grid hybrid system, 11% of the generated electricity (962 kWh) is provided by the wind turbine, while 85% (7126 kWh) is generated by the hydro turbine, with the remainder sourced from the main grid. Consequently, 2918 kWh of electricity is sold to the main grid annually, resulting in a saving of 1844 kg of CO_2 emissions annually. Additionally, as illustrated in Figure 25, in the hybrid system consisting of solar cells, hydro turbine, and the main grid, 20% of the electricity (1807 kWh) is supplied by the solar cells, while 77% (7126 kWh) is generated by the hydro turbine, with the remaining portion sourced from the main grid. By employing this system, 3679 kWh of electricity is sold to the grid annually, resulting in the prevention of CO_2 emissions by 2325 kg per year.

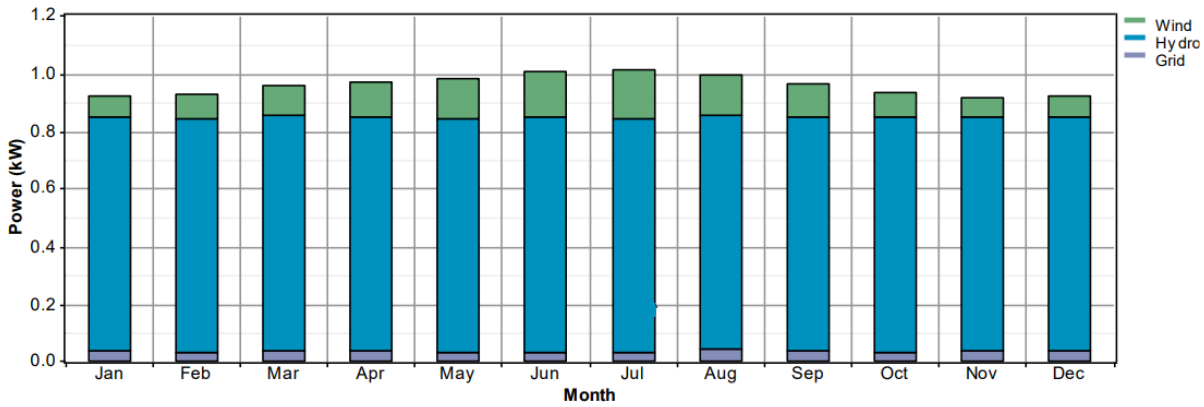

Fig. 24. Monthly average electric production for the wind-hydro system in scenario 2

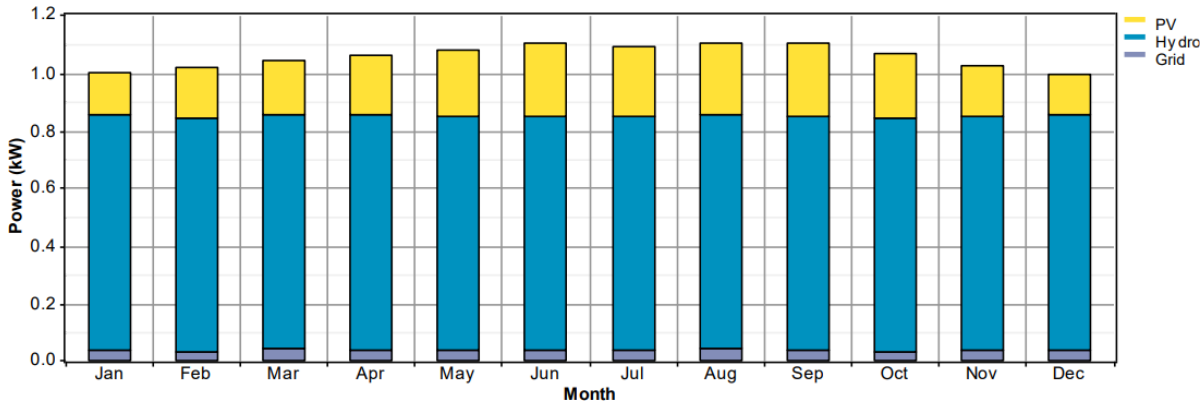

Fig. 25. Monthly average electric production for the solar-hydro system in scenario 2

In the second scenario, if no hydro turbine is utilized, based on the results presented in Table 4, the optimal configurations are as follows:

- Utilizing the main grid, which costs \$0.086 per kWh of electricity generated.
- Employing the main grid in combination with a wind turbine, costing \$0.28 per kWh of electricity.
- Utilizing the main grid in conjunction with solar cells, with a cost of \$0.346 per kWh of electricity.

In the second configuration (main grid plus wind turbine), 18% of the electricity (962 kWh/yr) is supplied by the wind turbine, while the remaining portion is sourced from the main grid. In the third configuration (main grid plus solar array), 33% of the electricity (1807 kWh/yr) is produced by the solar cells, with the rest being provided by the main grid.

8.3 Scenario no. 3: Grid-connected electricity and hydrogen generation

In this scenario, which utilizes hydrogen as an energy storage, electricity generators are similar to the first scenario, but the electricity grid has also been added to the electricity generators. In the third scenario, according to the results presented in Table 6, the hydro turbine-main grid configuration emerges as the most economically optimal state. In this configuration:

- The price per kWh of electricity generated is \$2.012.
- The price per kg of hydrogen generated is \$0.49.
- The total net present price is \$83,174.

Similar to the second scenario, the electricity generation section remains consistent, with 94% (7,126 kWh/y) of electricity being produced by the hydro turbine, as depicted in Figure 22. Additionally, in the most optimal state of the third scenario, a total of 31,025 kg of hydrogen is produced annually. Figure 26 illustrates the daily average hydrogen production, with the highest and lowest daily averages occurring in August (91.3 kg) and February (80.8 kg), respectively. The transaction of selling and buying electricity from/to the main grid follows the same pattern as observed in the second scenario.

In the optimal state of the third scenario, the absence of a generator is notable due to the continu-

ous availability of the main power grid throughout the day. Additionally, consistent with the observations in the first and second scenarios, the hybrid system incorporating a wind turbine demonstrates a lower total net present price compared to the solar-based hybrid system. However, it's worth mentioning that in terms of the price per kWh of electricity generation, the solar-based hybrid system offers a lower cost at \$1.831, whereas the wind turbine-based system incurs a slightly higher cost at \$1.954 in the third scenario.

In the most cost-efficient hybrid system based on a wind turbine in the third scenario, the price per kWh of power generated is \$1.954, the price per kg of hydrogen generated is \$0.523, and the total net present price is \$88639. Conversely, for the most cost-efficient hybrid system based on the solar array, these values are \$1.831, \$0.536, and \$90832, respectively.

Table 6. Simulation results for the third scenario.

Components	Total NPC (\$)	COE (\$/kWh)	COH (\$/kg)	Ren. Frac. (%)	CO_2 emission (kg/yr)
Hydro turbine, Grid	83174	2.012	0.490	94	−1297
Grid	84200	3.036	0.496	0	3206
Hydro turbine, Grid, Wind turbine, Converter	88639	1.954	0.523	96	−1844
Grid, Wind turbine, Converter	89665	3.201	0.529	17	2659
Hydro turbine, Grid, PV cell, Converter	90832	1.831	0.536	96	−2325
2178 31 0.542 3.163 91858 Grid, PV cell, Converter	91858	3.163	0.542	31	2178
Hydro turbine, Grid, Wind turbine, Converter, PV cell	94917	1.770	0.560	98	−2838

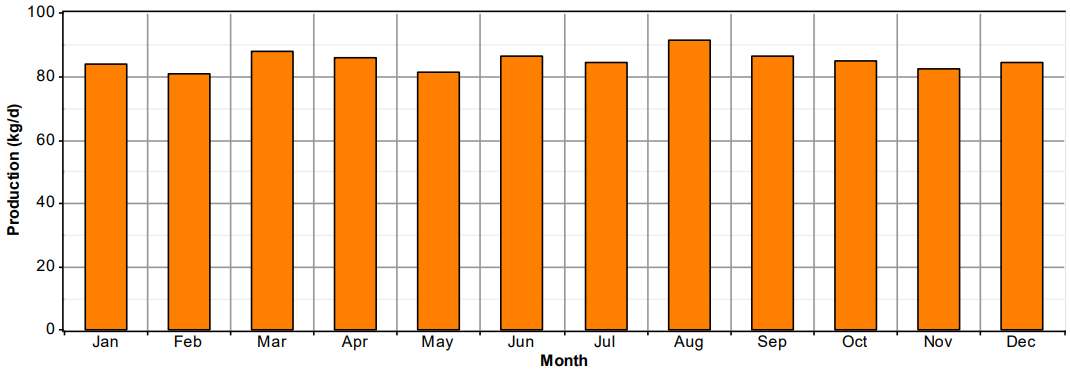

Fig. 26. Monthly average hydrogen production for the optimal state in the scenario 3

In the third scenario, if no hydro turbine is used in the hybrid system based on one renewable energy source, a combination of a wind turbine and the main grid is the most economical option. This configuration incurs a price per kWh of electricity generated, a price per kg of hydrogen generated, and a total net present price of \$3.201, \$0.529, and \$89665, respectively. However, the most cost-effective configuration for the third scenario, with a price per kWh of \$1.770, involves the combined use of a solar array and a wind turbine, along with a hydro turbine and the main grid.

Figure 27 provides a summary of the annual costs for the best configuration in the third scenario. The annual costs for the reformer and hydro turbine are \$14967 and \$362, respectively, while an annual revenue of \$115 is obtained through selling the electricity to the grid, similar to the second scenario. This results in a net annual cost of \$15214 for this hybrid system. The highest cost for the reformer is related to its fuel. Additionally, the Figure 27 illustrates that due to the availability of cheap fossil fuels in Iran, hydrogen production from renewable energies (using an electrolyzer) is not a cost-effective option.

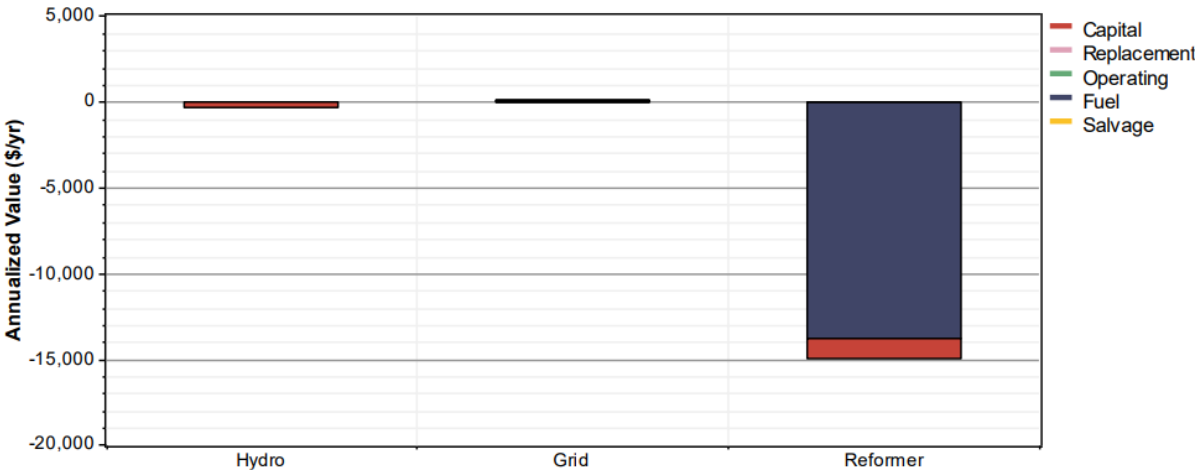

Fig. 27. Annualized cash flow summary for the optimal state in scenario 3

9 Conclusion

Despite the myriad benefits of Pico hydro, a comprehensive techno-economic-environmental study of this power generation method in Iran has been notably absent. Consequently, this study stands as the pioneering endeavor to conduct such a feasibility study, addressing the energy needs of a small village adjacent to the Koohrang tunnel in Chaharmahal and Bakhtiari province. Employing HOMER software, the study explores various grid-connected and off-grid scenarios, encompassing both electricity and hydrogen generation. Energy sources considered include hydro, solar, wind, diesel generator, and the main grid. The key findings are outlined below:

- In off-grid electricity generation scenarios, the most cost-effective option yields a price of $0.187 per kWh, achieved through a combination of hydro turbine, diesel generator, and battery.
- For grid-connected electricity generation, the lowest price per kWh stands at $0.033, achieved by integrating a hydro turbine with the main grid.
- The grid-connected electricity generation scenario sees an annual sale of 2053 kWh of surplus electricity to the main grid, resulting in savings of up to 1297 kg of CO_2 emissions.
- The lowest price per kg of hydrogen generation, at $0.49, is achieved through the utilization of a hydro turbine in conjunction with the main grid.
- In the grid-connected combined electricity and hydrogen generation scenario, the most economical option, priced at $1.77 per kWh of electricity generation, involves the use of a hydro turbine alongside the main grid, solar cells, and wind turbine.
- Across all studied scenarios, the hydro turbine consistently emerges as the most cost-effective option for electricity generation, with the wind turbine demonstrating economic superiority over solar cells.

Acknowledgement

The authors extend their gratitude to all the organizations that generously provided data for this research. Also, the authors express their appreciation to “Grammarly software” for skillfully refining the English language of the study.

References

[1] Izadyar N, Ong HC, Chong WT, Leong KY. Resource assessment of the renewable energy potential for a remote area: A review. Renewable and Sustainable Energy Reviews. 2016;62:908–923. Available from: https://www.sciencedirect.com/science/article/pii/S1364032116301150.

[2] Ozturk M, Bezir NC, Ozek N. Hydropower–water and renewable energy in Turkey: Sources and policy. Renewable and Sustainable Energy Reviews. 2009;13(3):605–615. Available from: https://www.sciencedirect.com/science/article/pii/S1364032107001499.

[3] Hoq T, Nawshad UA, Islam N, Syfullah K, Rahman R. Micro hydro power: promising solu-

tion for off-grid renewable energy source. International Journal of Scientific & Engineering Research. 2011;2(12):2–6.

[4] Cheng C, Liu B, Chau KW, Li G, Liao S. China's small hydropower and its dispatching management. Renewable and Sustainable Energy Reviews. 2015;42:43–55. Available from: https://www.sciencedirect.com/science/article/pii/S136403211400817X.

[5] Mondal MAH, Denich M. Assessment of renewable energy resources potential for electricity generation in Bangladesh. Renewable and Sustainable Energy Reviews. 2010;14(8):2401–2413. Available from: https://www.sciencedirect.com/science/article/pii/S1364032110001449.

[6] Abidin Z, Othman I. The future of hydropower in Malaysia. JURUTERA. 2005;p. 32–33.

[7] Kaldellis J, Kavadias K. Laboratory applications of renewable energy sources. Stamoulis, Athens. 2000;.

[8] Masters GM. Renewable and efficient electric power systems. John Wiley & Sons; 2013.

[9] IEA. Implementing agreement for hydro power technologies and programs. Paris, France; 2000.

[10] Kaunda CS, Kimambo CZ, Nielsen TK. Potential of Small-Scale Hydropower for Electricity Generation in Sub-Saharan Africa. ISRN Renewable Energy. 2012 Aug;2012:132606. Available from: https://doi.org/10.5402/2012/132606.

[11] Fadaeenejad M, Radzi MAM, AbKadir MZA, Hizam H. Assessment of hybrid renewable power sources for rural electrification in Malaysia. Renewable and Sustainable Energy Reviews. 2014;30:299–305. Available from: https://www.sciencedirect.com/science/article/pii/S1364032113007028.

[12] Nfah EM, Ngundam JM, Vandenbergh M, Schmid J. Simulation of off-grid generation options for remote villages in Cameroon. Renewable Energy. 2008;33(5):1064–1072. Available from: https://www.sciencedirect.com/science/article/pii/S096014810700211X.

[13] Boustani F. An assessment of the small hydropower potential of Sisakht region of Yasuj. World Academy of science, Engineering and technology. 2009;57:452–456.

[14] Nfah EM, Ngundam JM. Feasibility of pico-hydro and photovoltaic hybrid power systems for remote villages in Cameroon. Renewable Energy. 2009;34(6):1445–1450. Available from: https://www.sciencedirect.com/science/article/pii/S096014810800387X.

[15] Sen R, Bhattacharyya SC. Off-grid electricity generation with renewable energy technologies in India: An application of HOMER. Renewable Energy. 2014;62:388–398. Available from: https://www.sciencedirect.com/science/article/pii/S0960148113003832.

[16] Teixeira LE, Caux J, Beluco A, Bertoldo I, Louzada JAS, Eifler R. Feasibility study of a hydro PV hybrid system operating at a dam for water supply in southern Brazil. Journal of Power and Energy Engineering Irvine, CA Vol 3, n 9 (Sept 2015), p 70-83. 2015;.

[17] Ajao K, Ogunmokun A, Nangolo F, Shaanika S, Balogun O. Assessment of electro-mechanical components of bakolori small hydropower plant for refurbishment and modernization. ATBU Journal of Science, Technology and Education. 2017;4(3):30–38.

[18] Hammid AT, Sulaiman MHB, Abdalla AN. Prediction of small hydropower plant power production in Himreen Lake dam (HLD) using artificial neural network. Alexandria Engineering Journal. 2018;57(1):211–221. Available from: https://www.sciencedirect.com/science/article/pii/S111001681630343X.

[19] List of renewable and clean power plants built in the country;. http://www.satba.gov.ir/suna_content/media/image/2021/08/9069_orig.pdf.

[20] Resource protection through the development of renewable energy and electricity efficiency;. http://www.satba.gov.ir/suna_content/media/image/2021/08/9069_orig.pdf.

[21] Hosseini SE, Wahid MA. Hydrogen production from renewable and sustainable energy resources: Promising green energy carrier for clean development. Renewable and Sustainable Energy Reviews. 2016;57:850–866. Available from: https://www.sciencedirect.com/science/article/pii/S1364032115014951.

[22] Hanley ES, Deane J, Gallachóir BO. The role of hydrogen in low carbon energy futures–A review

of existing perspectives. Renewable and Sustainable Energy Reviews. 2018;82:3027–3045. Available from: https://www.sciencedirect.com/science/article/pii/S1364032117314089.

[23] Touili S, Alami Merrouni A, Azouzoute A, El Hassouani Y, illah Amrani A. A technical and economical assessment of hydrogen production potential from solar energy in Morocco. International Journal of Hydrogen Energy. 2018;43(51):22777–22796. Available from: https://www.sciencedirect.com/science/article/pii/S0360319918333639.

[24] Pellow MA, Emmott CJ, Barnhart CJ, Benson SM. Hydrogen or batteries for grid storage? A net energy analysis. Energy & Environmental Science. 2015;8(7):1938–1952.

[25] Nasiri M, Ramazani Khorshid-Doust R, Bagheri Moghaddam N. The status of the hydrogen and fuel cell innovation system in Iran. Renewable and Sustainable Energy Reviews. 2015;43:775–783. Available from: https://www.sciencedirect.com/science/article/pii/S1364032114010144.

[26] Rezaei M, Khalilpour KR, Jahangiri M. Multi-criteria location identification for wind/solar based hydrogen generation: The case of capital cities of a developing country. International Journal of Hydrogen Energy. 2020;45(58):33151–33168. Available from: https://www.sciencedirect.com/science/article/pii/S0360319920335783.

[27] Rezaei M, Mostafaeipour A, Jahangiri M. Economic assessment of hydrogen production from sea water using wind energy: a case study. Wind Engineering. 2021;45(4):1002–1019.

[28] Jahangiri M, Karimi Shahmarvandi F, Alayi R. Renewable Energy-Based Systems on a Residential Scale in Southern Coastal Areas of Iran: Trigeneration of Heat, Power, and Hydrogen. Journal of Renewable Energy and Environment. 2021;8(4):67–76. Available from: https://www.jree.ir/article_135328.html.

[29] Almutairi K, Mostafaeipour A, Baghaei N, Techato K, Chowdhury S, Jahangiri M, et al. Techno-Economic Investigation of Using Solar Energy for Heating Swimming Pools in Buildings and Producing Hydrogen: A Case Study. Frontiers in Energy Research. 2021;9. Available from: https://www.frontiersin.org/articles/10.3389/fenrg.2021.680103.

[30] Rezaei M, Jahangiri M, Razmjoo A. Utilization of Rooftop Solar Units to Generate Electricity and Hydrogen: A Technoeconomic Analysis. International Journal of Photoenergy. 2021 Nov;2021:8858082. Available from: https://doi.org/10.1155/2021/8858082.

[31] Mostafaeipour A, Jahangiri M, Saghaei H, Raiesi Goojani A, Chowdhury MS, Techato K. Impact of Different Solar Trackers on Hydrogen Production: A Case Study in Iran. International Journal of Photoenergy. 2022 Oct;2022:3186287. Available from: https://doi.org/10.1155/2022/3186287.

[32] Jahangiri M, Rezaei M, Mostafaeipour A, Goojani AR, Saghaei H, Hosseini Dehshiri SJ, et al. Prioritization of solar electricity and hydrogen co-production stations considering PV losses and different types of solar trackers: A TOPSIS approach. Renewable Energy. 2022;186:889–903. Available from: https://www.sciencedirect.com/science/article/pii/S0960148122000556.

[33] Hay JXW, Wu TY, Juan JC, Md Jahim J. Biohydrogen production through photo fermentation or dark fermentation using waste as a substrate: Overview, economics, and future prospects of hydrogen usage. Biofuels, Bioproducts and Biorefining. 2013;7(3):334–352. Available from: https://onlinelibrary.wiley.com/doi/abs/10.1002/bbb.1403.

[34] Kalbasi R, Jahangiri M, Tahmasebi A. Comprehensive Investigation of Solar-Based Hydrogen and Electricity Production in Iran. International Journal of Photoenergy. 2021 Jun;2021:6627491. Available from: https://doi.org/10.1155/2021/6627491.

[35] Benefits of Grid-Tied and Off-Grid Solar Power Systems;. Accessed: 20 Mar 2019. https://www.solarreviews.com/news/.

[36] Aziz AS, Tajuddin MFN, Adzman MR, Ramli MAM, Mekhilef S. Energy Management and Optimization of a PV/Diesel/Battery Hybrid Energy System Using a Combined Dispatch Strategy. Sustainability. 2019;11(3). Available from: https://www.mdpi.com/2071-1050/11/3/683.

[37] Jahangiri M, Khosravi A, Raiesi HA, Mostafaeipour A. Analysis of standalone PV-based hybrid systems for power generation in Rural area. In: International conference on

fundamental research in electrical engineering; 2017. p. 1–10.

[38] Hossain CA, Chowdhury N, Longo M, Yaïci W. System and Cost Analysis of Stand-Alone Solar Home System Applied to a Developing Country. Sustainability. 2019;11(5). Available from: https://www.mdpi.com/2071-1050/11/5/1403.

[39] Jahangiri M, Shamsabadi AA, Riahi R, Raeiszadeh F, Dehkordi PF. Levelized Cost of Electricity for Wind-Solar Power Systems in Japan, a Review. Journal of Power Technologies. 2020;100(3):188–210. Available from: https://papers.itc.pw.edu.pl/index.php/JPT/article/view/1359.

[40] Ramli MAM, Hiendro A, Twaha S. Economic analysis of PV/diesel hybrid system with flywheel energy storage. Renewable Energy. 2015;78:398–405. Available from: https://www.sciencedirect.com/science/article/pii/S0960148115000348.

[41] Brecl K, Topič M. Energy and Economic Yield of Photovoltaic Systems: Reactive-Power Impact. Electrotechnical Review/Elektrotehniski Vestnik. 2014;81.

[42] Jahangiri M, Nematollahi O, Haghani A, Raiesi HA, Shamsabadi AA. An optimization of energy cost of clean hybrid solar-wind power plants in Iran. International Journal of Green Energy. 2019;16(15):1422–1435. Available from: https://doi.org/10.1080/15435075.2019.1671415.

[43] Moein M, Pahlavan S, Jahangiri M, Alidadi Shamsabadi A. Finding the Minimum Distance from the National Electricity Grid for the Cost-Effective Use of Diesel Generator-Based Hybrid Renewable Systems in Iran. Journal of Renewable Energy and Environment. 2018;5(1):8–22. Available from: https://www.jree.ir/article_88377.html.

[44] Aziz AS, Tajuddin MFN, Adzman MR, Azmi A, Ramli MAM. Optimization and sensitivity analysis of standalone hybrid energy systems for rural electrification: A case study of Iraq. Renewable Energy. 2019;138:775–792. Available from: https://www.sciencedirect.com/science/article/pii/S096014811930148X.

[45] Mostafaeipour A, Rezaei M, Jahangiri M, Qolipour M. Feasibility analysis of a new tree-shaped wind turbine for urban application: A case study. Energy & Environment. 2020;31(7):1230–1256.

[46] Lambert T. HOMER Help. HOMER ENERGY, May. 2004;6.

[47] Jahangiri M, Mostafaeipour A, Rahman Habib HU, Saghaei H, Waqar A. Effect of Emission Penalty and Annual Interest Rate on Cogeneration of Electricity, Heat, and Hydrogen in Karachi: 3E Assessment and Sensitivity Analysis. Journal of Engineering. 2021 Apr;2021:6679358. Available from: https://doi.org/10.1155/2021/6679358.

[48] Das BK, Zaman F. Performance analysis of a PV/Diesel hybrid system for a remote area in Bangladesh: Effects of dispatch strategies, batteries, and generator selection. Energy. 2019;169:263–276. Available from: https://www.sciencedirect.com/science/article/pii/S0360544218323806.

[49] Global petrol prices, Diesel prices, liter; 2019. Accessed: 29 Mar 2019. https://www.globalpetrolprices.com/diesel_prices/.

[50] Trading economics. Interest Rate, Asia; 2019. Accessed: 29 Mar 2019. https://tradingeconomics.com/country-list/interest-rate?continent=asia/.

[51] Ebrahimi S, Jahangiri M, Raiesi HA, Ariae AR. Optimal Planning of On-Grid Hybrid Microgrid for Remote Island Using HOMER Software, Kish in Iran. International Journal of Energetica. 2019;3(2):13–21. Available from: https://www.ijeca.info/index.php/IJECA/article/view/77.

[52] Jahangiri M, Haghani A, Alidadi Shamsabadi A, Mostafaeipour A, Pomares LM. Feasibility study on the provision of electricity and hydrogen for domestic purposes in the south of Iran using grid-connected renewable energy plants. Energy Strategy Reviews. 2019;23:23–32. Available from: https://www.sciencedirect.com/science/article/pii/S2211467X18301159.

[53] Abdali T, Pahlavan S, Jahangiri M, Alidadi Shamsabadi A, Sayadi F. Techno-Econo-Environmental study on the use of domestic-scale wind turbines in Iran. Energy Equipment and Systems. 2019;7(4):317–338. Available from: https://www.energyequipsys.com/article_37669.html.

[54] Basir Khan MR, Jidin R, Pasupuleti J, Shaaya SA. Optimal combination of solar, wind, micro-hydro and diesel systems based on actual seasonal load profiles for a resort island in the

South China Sea. Energy. 2015;82:80–97. Available from: https://www.sciencedirect.com/science/article/pii/S0360544215000043.

[55] Ariae AR, Jahangiri M, Fakhr MH, Shamsabadi AA. Simulation of biogas utilization effect on the economic efficiency and greenhouse gas emission: a case study in Isfahan, Iran. International Journal of Renewable Energy Development. 2019;8(2):149–160.

[56] Jahangiri M, Haghani A, Heidarian S, Alidadi Shamsabadi A, Pomares LM. Electrification of a Tourist Village Using Hybrid Renewable Energy Systems, Sarakhiyeh in Iran. Journal of Solar Energy Research. 2018;3(3):201–211. Available from: https://jser.ut.ac.ir/article_68643.html.

[57] Padrón I, Avila D, Marichal GN, Rodríguez JA. Assessment of Hybrid Renewable Energy Systems to supplied energy to Autonomous Desalination Systems in two islands of the Canary Archipelago. Renewable and Sustainable Energy Reviews. 2019;101:221–230. Available from: https://www.sciencedirect.com/science/article/pii/S136403211830741X.

[58] Pahlavan S, Jahangiri M, Alidadi Shamsabadi A, Rahimi Ariae A. Assessment of PV-Based CHP System: The Effect of Heat Recovery Factor and Fuel Type. Journal of Energy Management and Technology. 2019;3(1):40–47. Available from: https://www.jemat.org/article_78129.html.

[59] Teimourian A, Bahrami A, Teimourian H, Vala M, Oraj Huseyniklioglu A. Assessment of wind energy potential in the southeastern province of Iran. Energy Sources, Part A: Recovery, Utilization, and Environmental Effects. 2020;42(3):329–343. Available from: https://doi.org/10.1080/15567036.2019.1587079.